



## RESEARCH ARTICLE

WILEY

# Thermo-erosional valleys in Siberian ice-rich permafrost

Anne Morgenstern<sup>1</sup> | Pier Paul Overduin<sup>1</sup> | Frank Günther<sup>1,2,3</sup> |  
 Samuel Stettner<sup>1,2,4</sup> | Justine Ramage<sup>1,2,5</sup> | Lutz Schirrmeister<sup>1</sup> |  
 Mikhail N. Grigoriev<sup>6,7,8</sup> | Guido Grosse<sup>1,2</sup>

<sup>1</sup>Department of Permafrost Research, Alfred Wegener Institute Helmholtz Centre for Polar and Marine Research, Potsdam, Germany<sup>2</sup>Institute of Geosciences, University of Potsdam, Potsdam, Germany<sup>3</sup>Faculty of Geography, Laboratory Geoecology of the North, Lomonosov Moscow State University, Moscow, Russia<sup>4</sup>Department Earth Observation, German Aerospace Center – Space Administration, Bonn, Germany<sup>5</sup>Nordregio, Nordic and European research centre for regional development and planning, Stockholm, Sweden<sup>6</sup>Melnikov Permafrost Institute, Siberian Branch, Russian Academy of Sciences, Yakutsk, Russia<sup>7</sup>Trofimuk Institute for Petroleum Geology and Geophysics, Siberian Branch, Russian Academy of Sciences, Novosibirsk, Russia<sup>8</sup>North-Eastern Federal University, Yakutsk, Russia**Correspondence**

Anne Morgenstern, Alfred Wegener Institute Helmholtz Center for Polar and Marine Research, Department of Permafrost Research, Telegrafenberg A45, 14473, Potsdam, Germany.  
 Email: anne.morgenstern@awi.de

**Funding information**

Christiane Nüsslein-Volhard Foundation; European Research Council, Grant/Award Number: 338335; German Academic Exchange Service DAAD P.R.I.M.E., Grant/Award Number: 605728; Helmholtz-Gemeinschaft, Grant/Award Numbers: PD-003, VH-NG-801; Polar Geospatial Center, NSF-OPP awards, Grant/Award Numbers: 1043681, 1542736, 1559691; RapidEye Science Archive (RESA); Russian Foundation for Basic Research, Grant/Award Numbers: 18-05-70091, 18-45-140057; Studienstiftung des Deutschen Volkes; Universität Potsdam; BMBF KoPf, Grant/Award Number: #03F0764B

**Abstract**

Thermal erosion is a major mechanism of permafrost degradation, resulting in characteristic landforms. We inventory thermo-erosional valleys in ice-rich coastal lowlands adjacent to the Siberian Laptev Sea based on remote sensing, Geographic Information System (GIS), and field investigations for a first regional assessment of their spatial distribution and characteristics. Three study areas with similar geological (Yedoma Ice Complex) but diverse geomorphological conditions vary in valley areal extent, incision depth, and branching geometry. The most extensive valley networks are incised deeply (up to 35 m) into the broad inclined lowland around Mamontov Klyk. The flat, low-lying plain forming the Buor Khaya Peninsula is more degraded by thermokarst and characterized by long valleys of lower depth with short tributaries. Small, isolated Yedoma Ice Complex remnants in the Lena River Delta predominantly exhibit shorter but deep valleys. Based on these hydrographical network and topography assessments, we discuss geomorphological and hydrological connections to erosion processes. Relative catchment size along with regional slope interact with other Holocene relief-forming processes such as thermokarst and neotectonics. Our findings suggest that thermo-erosional valleys are prominent, hitherto overlooked permafrost degradation landforms that add to impacts on biogeochemical cycling, sediment transport, and hydrology in the degrading Siberian Yedoma Ice Complex.

**KEYWORDS**

geomorphology, periglacial landscapes, permafrost degradation, thermal erosion, valley distribution, Yedoma Ice Complex

This is an open access article under the terms of the Creative Commons Attribution License, which permits use, distribution and reproduction in any medium, provided the original work is properly cited.

© 2020 The Authors. Permafrost and Periglacial Processes published by John Wiley & Sons Ltd

## 1 | INTRODUCTION

Climate warming in the Arctic is occurring at a much faster rate than the global average,<sup>1</sup> impacting polar permafrost regions. Permafrost warming and erosion of permafrost deposits have been reported throughout the northern high latitudes.<sup>2–4</sup> Thermokarst and thermal erosion are two major processes of ice-rich permafrost degradation in periglacial landscapes. They result in thawing of permafrost-stored organic carbon, which then can decompose and be released to the atmosphere and the hydrological system.<sup>5–8</sup> Landscapes affected by thermokarst and thermal erosion are estimated to contain ~330 Pg carbon in the upper 3 m subsurface, constituting ~30% of the total 0–3 m permafrost region soil organic carbon storage (1,073 Pg C), highlighting their importance for the global carbon cycle in a rapidly warming Arctic.<sup>9,10</sup> The two processes may also substantially alter the water and energy balances of affected regions.<sup>11,12</sup>

Thermal erosion is defined as the erosion of ice-bearing permafrost by the combined thermal and mechanical action of moving water.<sup>13</sup> Whereas thermokarst is an *in situ* process including melting of ground ice followed by surface subsidence but without hydraulic transport of earth materials, thermal erosion is a dynamic process involving the wearing away by thermal means (i.e., the melting of ice) and by mechanical means (i.e., hydraulic transport).<sup>13</sup> Two types of thermal erosion can be distinguished: linear or vertical thermal erosion, which acts to depth, and lateral thermal erosion, which acts sideways.<sup>14,15</sup>

Thermokarst processes occur mostly in flat lowland terrain with low hydraulic gradient; the resulting characteristic landforms are thermokarst lakes, thermokarst depressions (alasses), and thermokarst mounds. Thermal erosion takes place along river banks<sup>16–20</sup> and coastlines,<sup>21,22</sup> at the shores of lakes,<sup>23,24</sup> but also in lowlands with abundant ground ice and sufficient gradients to allow for channelized surface water flow.<sup>25</sup> Here, it can result in the formation of thermo-erosional gullies<sup>26–29</sup> or even large thermo-erosional valleys and valley systems. Thermal erosion, thermokarst, and the landforms resulting from these processes interact with each other, as thermo-erosional gullies and valleys can supply water to thermokarst lakes and basins<sup>30,31</sup> and enlarge thermokarst depressions.<sup>32</sup> At the same time, they may also inhibit thermokarst activity by drainage of flat uplands and breaching of thermokarst lakes.<sup>33–36</sup>

In contrast to thermokarst lakes, which have been investigated in numerous studies, for example as sources of carbon release to the atmosphere,<sup>5,6</sup> with respect to spatial distribution patterns,<sup>37</sup> or as indicators of a changing water balance in permafrost regions,<sup>38,39</sup> only a few studies are available on thermo-erosional gullies and valleys or discuss the interaction of thermal erosion with thermokarst under differing regional relief conditions. Thermo-erosional valleys have been described in the Lena River Delta<sup>33</sup> and mapped in two regions of the East Siberian coastal lowlands in the context of an overall quantification of thermokarst-affected terrain types.<sup>30,40</sup> Other studies have reported rapid formation and growth of thermo-erosional gullies due to thawing permafrost.<sup>26–29,41</sup> Gullies and valleys can deeply erode underlying deposits in a short time and therefore increase sediment

and nutrient delivery to rivers, lakes, and the sea.<sup>32,41,42</sup> They also may reconfigure drainage networks, thereby leading to large changes in runoff volume and timing.<sup>43</sup> Thermo-erosional gullies and valleys are common in Arctic landscapes, act as important snow accumulation areas, and alter the water, sediment, and organic matter transport from inland permafrost to receiving waters at the local scale. Yet, there are no systematic studies available that classify and quantify thermo-erosional valleys and their impacts at the Arctic scale or that analyze differences in valley network characteristics across different permafrost regions.

As a first step to fill this gap, we provide here an overview of thermo-erosional valleys and their role in the degradation of ice-rich permafrost in the eastern Siberian Arctic. The specific objectives of this study are: (a) to describe the morphometry and spatial distribution of thermo-erosional valleys across three Laptev Sea coastal lowland regions based on remote sensing, geoinformation, and field data; and (b) to relate the identified spatial patterns and morphologies to the topographical and cryolithological settings of the study areas and their evolution through the Holocene. In particular, we address the following questions: How abundant are thermo-erosional landforms in the study region? Which drainage patterns and valley types occur? How do the valleys and their networks differ between the study areas and why? and we propose a conceptual model for valley evolution in the study region during the Holocene.

## 2 | REGIONAL SETTING

This study focuses on three sites bordering the Siberian Laptev Sea coast (Figure 1). The stratigraphy in all three study areas is comparable and consists of late Pleistocene polygenetic Yedoma Ice Complex deposits underlain by middle to late Pleistocene sandy deposits and covered by various Holocene deposits.<sup>44–52</sup> The Yedoma Ice Complex is 10–40 m thick and consists of ice-supersaturated silty to sandy sediments and buried cryosols. Large syngenetic ice wedges of up to several tens of meters thickness truncate the sediment column and contribute to a total ground-ice volume of up to 80%. All three sites are situated in the Arctic tundra zone<sup>53</sup> and in the continuous permafrost zone with several hundreds of meters permafrost thickness and mean annual ground temperatures from  $-9$  to  $< -11^{\circ}\text{C}$ .<sup>15</sup>

The western site around Cape Mamontov Klyk belongs to the Olenyok–Anabar coastal lowland. It is bordered by the Pronchishchev Ridge to the south and is inclined slightly in the NNE direction towards the Laptev Sea.<sup>30</sup> The central site in the Lena River Delta is composed of insular Yedoma remnants and, together with a few locations of bedrock outcrops, they constitute the third geomorphological main terrace of the delta, which accounts for 5.9% of the total delta area of 29,000 km<sup>2</sup>. The second main terrace consists of fluvial sandy deposits and covers 21% of the Lena Delta area. The third and second terraces represent late Pleistocene non-deltaic units, whereas the Holocene deltaic deposits are considered the first geomorphological main terrace of the Lena Delta.<sup>33,34,45,47,54</sup> The eastern site, the Buor Khaya Peninsula, is the westernmost part of the Yana–Indigirka

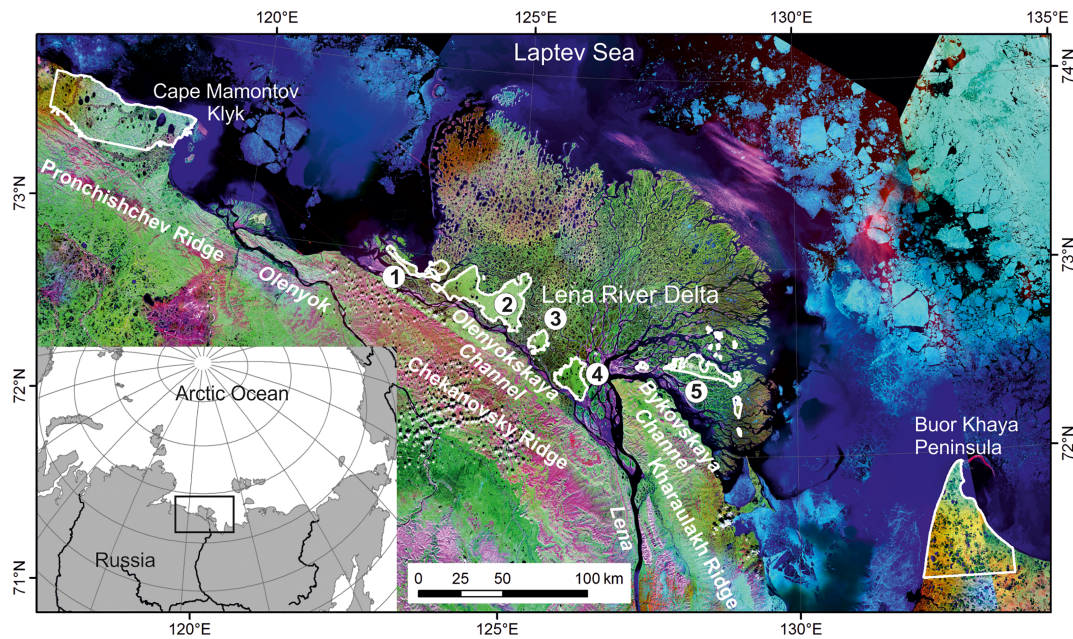


**FIGURE 1** Regional setting of the study areas (Landsat-7 ETM + mosaic; GeoCover<sup>TM</sup> 2000). White outlines mark the spatial extent of individual study areas. 1 – Ebe-Basyn Island, 2 – Khardang Island, 3 – Dzhangylakh Island, 4 – Kurungnakh Island, 5 – Sobo-Sise Island [Colour figure can be viewed at [wileyonlinelibrary.com](http://wileyonlinelibrary.com)]

coastal lowland. In contrast to the other sites, the base of the Yedoma Ice Complex deposits is below modern sea level (b.s.l.) here and is currently not exposed. Coring about 800 m off the western shore indicates its location at about 4 m b.s.l. followed by Pleistocene sands that extend down to at least 52 m b.s.l.<sup>55,56</sup>

Holocene deposits of 1–2 m thickness cover the Yedoma Ice Complex deposits. Holocene deposits are also found in thermokarst depressions and in river and thermo-erosional valleys. They consist of peat, silty to sandy sediments with high organic matter and ice content, and lacustrine silty sediments.<sup>57</sup> The high ice content and large thickness (10–40 m) of the Yedoma Ice Complex deposits cause substantial terrain subsidence due to thawing and has provided the conditions for widespread surface changes from thermokarst and thermal erosion since the Lateglacial/Holocene transition about 12–10 ka BP.<sup>35,58</sup>

### 3 | MATERIAL AND METHODS

The thermo-erosional valleys analyzed in this study were manually digitized from topographic maps as well as Hexagon, Landsat-7 and RapidEye satellite imagery as line features in a Geographic Information System (GIS) using ESRI ArcGIS (Table 1). The dataset is available in the PANGAEA open-access archive.<sup>59</sup> It includes thermo-erosional gullies and valleys as well as streams and rivers, as development of all of these features potentially involved thermo-erosional processes at some stage given the high ground-ice content of both surface types, Yedoma Ice Complex and Holocene deposits, upon which they formed. The main criterion for the mapping of linear features from

satellite imagery as thermo-erosional valleys and gullies was their clear incision into the surface with visible bank slopes, expressed as contrast in reflectance between the slopes and the surrounding surface.

Spatial analyses in GIS included the calculation of spatial statistics and summary metrics for each study area, including total stream length, drainage density and valley density, as well as derivation of exemplary valley profiles from ArcticDEM, a high-resolution Digital Elevation Model (DEM) of the Arctic. Drainage density is defined as the total length of streams divided by the area of their drainage basin.<sup>60,61</sup> On Cape Mamontov Klyk and on the Buor Khaya Peninsula, some of the streams and valleys and their catchment areas are truncated by the southern study area boundary. We nevertheless included them in our calculations, implicitly assuming that the truncated portions had similar drainage network densities to the portions included in the study area. In this study, drainage density was thus defined as the total length of all streams and rivers divided by the total study area. In addition, valley density was calculated, because large valleys often have well-developed floodplains with strongly meandering streams, and a meandering stream has a greater length than its valley. The valley floodplains were delineated as polygonal features along the valley floor margins, and their center line was digitized to determine valley length in comparison to stream length. Valley density was then calculated as the sum of rivers, streams, and intermittent streams outside valley floodplains and the valley floodplain centerlines divided by the total area of the study area. Figure S1 provides an illustration of the difference between drainage density and valley density and their calculation.

We used GIS datasets from previous studies on Cape Mamontov Klyk<sup>30</sup> and in the Lena Delta<sup>34</sup> to quantify the area affected by

**TABLE 1** Overview of the spatial properties of the data sources used for the compilation of the dataset of thermo-erosional landforms analyzed in this study<sup>59</sup>

Location	Source data for digitization of thermo-erosional landforms	Year	Map scale; ground resolution	
Cape Mamontov Klyk	Rivers, streams, intermittent streams	Topographic maps	1970s	1:100,000
	Smaller gullies and valleys not captured in the topographic maps	Landsat-7 ETM+, pan	2000	15 m
Lena River Delta	Thermo-erosional landforms	Hexagon	1975	10 m
		Landsat-7 ETM + mosaic	2000, 2001	30 m
		Hexagon mosaic	1975	10 m
Buor Khaya Peninsula	Thermo-erosional landforms	Rapid eye	2010	6.5 m

thermokarst in order to assess the spatial relationship between thermo-erosional landforms and thermokarst lakes and basins and to discuss differences in the predominance of the degradation type between the study areas in light of regional relief development. On the Buor Khaya Peninsula, only thermokarst lakes could be delineated (and not basins), because thermokarst was so widespread that individual basin boundaries intersected and could not be distinguished unambiguously. Therefore, the lake area represents an underestimate of the thermokarst-affected area for the Buor Khaya Peninsula, which excludes larger dry basins.

Field observations and measurements of thermo-erosional and fluvial landforms were collected during field campaigns to Cape Mamontov Klyk in 2003,<sup>30,62</sup> to the western Lena Delta in 2005 and 2013,<sup>63,64</sup> to Kurungnakh Island in 2008 and in 2013–2018,<sup>35,65,66</sup> and to the Buor Khaya Peninsula in 2010.<sup>51</sup> In 2013, 2016, and 2017, valley profiles were measured on Khardang, Kurungnakh and Sobo-Sise islands with a survey-grade global navigation satellite system (GNSS Leica Viva GS10/15) operated in real-time kinematic mode in 2013 and in static phase observation mode in 2016 and 2017.

Terrain analyses and the extraction of valley transverse profiles were performed using the ArcticDEM, which is based on stereophotogrammetrically derived elevations from sub-meter-resolution satellite imagery.<sup>67</sup> We used mosaic tiles of Release 6, v2.0 with a 5-m resolution that were averaged from multiple 2-m-resolution strip DEMs and provide a consistent data source over large areas. The suitability of the ArcticDEM to extract thermo-erosional valley profile characteristics has been confirmed by comparing GNSS-measured valley profiles with those extracted from the ArcticDEM at the same locations (Figure S2).

## 4 | RESULTS

The summary characteristics of the three study sites are given in Table 2. Cape Mamontov Klyk is extensively covered with valleys and streams (Figure 2) and therefore has the highest drainage density (2.0). The drainage densities for the Lena Delta and Buor Khaya Peninsula are lower (0.9 and 1.0, respectively). Valley densities are

similar or equal to the drainage densities, implying that meandering streams in wide floodplains represent only a small proportion of the drainage system in each study area, which is also indicated by their low percentages of floodplain area.

### 4.1 | Drainage patterns of thermo-erosional valley networks

Cape Mamontov Klyk is characterized by extensive valley networks (Figure 2a). They start on and route across the Yedoma uplands and end at the coast. Some of them cross the whole study area from the Pronchishchev Ridge in the south to the Laptev Sea coast in the north. Smaller networks also start or end in thermokarst lakes and alasses. The network patterns vary from dendritic to pinnate and trellis-like drainage (Figure 3a, b). In the pinnate and trellis-like drainage form, short, straight, almost parallel headwater channels join the long, low-gradient valley channels at acute and right angles, respectively.

In the Lena River Delta, extensive dendritic and pinnate to trellis-like valley networks occur only on Khardang Island (Figure 2b), which is the largest and highest part of the delta's third terrace, exhibiting the greatest distance between its interior and the margins. Most common in the Lena Delta are short thermo-erosional valleys (up to 2 km long, sometimes with short tributary valleys) that run roughly perpendicular to the edges of the islands, where steep cliffs form an abrupt transition between the Yedoma uplands and the delta channels and their floodplains (Figure 3c). Longer valleys often interconnect alasses and discharge into the delta channels. They can be several kilometers long and have several tributary valleys or streams (Figure 3d).

All these valley types also occur on the Buor Khaya Peninsula. However, the predominant type here are long valleys and streams that extend from the interior to the coast. They have an irregular course following the ice-wedge polygonal pattern of the deposits, in which they formed (Figures 2c, 3e). They do bifurcate, but at intervals of several kilometers. In between they feature frequent, very short (a few hundred meters long), parallel-sided valleys almost perpendicular to the main valley. In some areas this pattern resembles a trellis-like form; in areas where the tributaries bend along the polygonal

**TABLE 2** Summary characteristics of the three study sites and their thermo-erosional and thermokarst landforms

	Cape Mamontov Klyk	Lena Delta	Buor Khaya Peninsula
Study area (km <sup>2</sup> )	2,109	1,690	2,001
Max. relief height (m a.s.l.)	75.5	66	65
Min. relief height (m a.s.l.)	0	0	0
Min. distance between highest and lowest relief parts (km)	22	7	7
Total stream length (km) <sup>a</sup>	4,153	1,541	2,047
Drainage density (km/km <sup>2</sup> )	2.0	0.9	1.0
Valley floodplains (km <sup>2</sup> )	203.8	8.2	25.6
Floodplain area percentage of study site (%)	9.7	0.5	1.3
Maximum floodplain width (km)	4.5	1	1.5
Total length of valley floodplain centerlines (km)	199	25	38
Max. valley depth (m)	35	35	25
Total valley length (km) <sup>b</sup>	3,877	1,541	1,954
Valley density (km/km <sup>2</sup> )	1.8	0.9	1.0
Alases (km <sup>2</sup> )	418.2 <sup>d</sup>	337.7 <sup>e</sup>	n.d.
Thermokarst lakes (km <sup>2</sup> )	158.2 <sup>d</sup>	88.3 <sup>e</sup>	192.9
Thermokarst lakes on Yedoma uplands (km <sup>2</sup> )	23.0 <sup>d</sup>	37.4 <sup>e</sup>	n.d.
Total area affected by thermokarst lakes and alases (km <sup>2</sup> ) <sup>c</sup>	441.2 <sup>d</sup>	375.1 <sup>e</sup>	n.d.
Thermokarst areal percentage of study site (%)	20.9 <sup>d</sup>	22.2 <sup>e</sup>	n.d.

<sup>a</sup>Calculated as the sum of all rivers, streams, and intermittent streams.

<sup>b</sup>Calculated as the sum of rivers, streams, and intermittent streams outside valley floodplains and the valley floodplain centerlines.

<sup>c</sup>Calculated as the sum of thermokarst lakes on Yedoma uplands and thermokarst basins.

<sup>d</sup>Data based on Grosse et al. (2006).<sup>30</sup>

<sup>e</sup>Data from Morgenstern et al. (2011).<sup>34</sup>

n.d. – not determined due to lack of data for alas extent.

network at almost right angles further upstream, it shows rectangular-like forms. These valley systems occur on the few remaining Yedoma uplands as well as in the extensive flat and lower elevation areas that have resulted from thermokarst subsidence. Sometimes they even start in low areas and then cut through Yedoma remnants that are elevated up to 20 m above these low areas.

In all three study areas, straight, short gullies are often radially located around alases and thermokarst lakes (Figure 3f). They start on the Yedoma uplands, cut into the slopes, and end abruptly at the foot of the alas slope or at the lake level.

## 4.2 | Valley and stream channel morphology

The valley profiles are similar in all three study areas. Short tributary valleys typically have a straight longitudinal course (low sinuosity) (Figure 3) with a moderate gradient and V-shaped transverse profiles (Figure 4d). Higher order and main valleys have a higher sinuosity (Figure 3a, b, e) and low gradient. Narrow valleys with a V- or U-shaped transverse profile meander at sharp angles, obviously following the ice-wedge polygonal network (Figure 3a, e). Broader valleys with a U-shaped transverse profile (Figure 4f) tend to straighten in their longitudinal course (lower sinuosity), but the streams on their floors are meandering with high sinuosity. The broad valleys with large floodplains (Figure 4g) have a smoothly meandering river and oxbow and small thermokarst lakes. The maximum widths of these valley floodplains are 4.5, 1.0, and 1.5 km in the Cape Mamontov Klyk, Lena Delta, and Buor Khaya Peninsula study areas, respectively. Streams in alases and some of the rivers in the large, flat, low-elevation areas of the Buor Khaya Peninsula meander and are often only up to a few meters indented into the surface. The maximum valley depth measured in any transverse ArcticDEM profile is about 35, 35, and 25 m in the Cape Mamontov Klyk, Lena Delta, and Buor Khaya Peninsula study area, respectively (Table 2).

## 4.3 | Categorization of thermo-erosional valleys

Based on the results of spatial analyses and field observations (Figure 5) we categorize the thermo-erosional landforms in the study area into the following types (Table 3):

1. Short, straight gullies around thermokarst lakes and alases cut down to 10 m deep into the slopes of the thermokarst features and mostly follow the same gradient as the slope, as indicated by the uniform width of the bank slopes along the gullies (Table 3a, Figure 4a). They are densely covered with more vital and higher growing wet sedge tundra vegetation than the surrounding slope sections.

2. In alases, small streams often occur as drainage pathways and connect residual and secondary thermokarst lakes on the alas floor with the hydrological system outside the alases. In cases of catastrophic drainage of large thermokarst lakes, the draining water cuts outflow channels into the unfrozen soft sediments at the lake bottom that persist as valleys on the floor of the newly formed alas and that can reach 20 m depth (Table 3b, Figure 4b).

3. Deep V-shaped ravines (Table 3c, Figure 4c) were observed along the cliffs of Cape Mamontov Klyk and the Lena Delta Yedoma Ice Complex islands (Figure 5f) and along the coasts of the Buor Khaya Peninsula (Figure 5g). They have a steep gradient, because they descend from the Yedoma uplands with elevations of up to 50 m to river or sea level over a short distance of only a few tens to hundreds of meters. Their lower bank slopes and floors are characterized by strong soil disturbance and active erosion and often are free of vegetation. Some of these ravines have formed due to the drainage of thermokarst lakes.

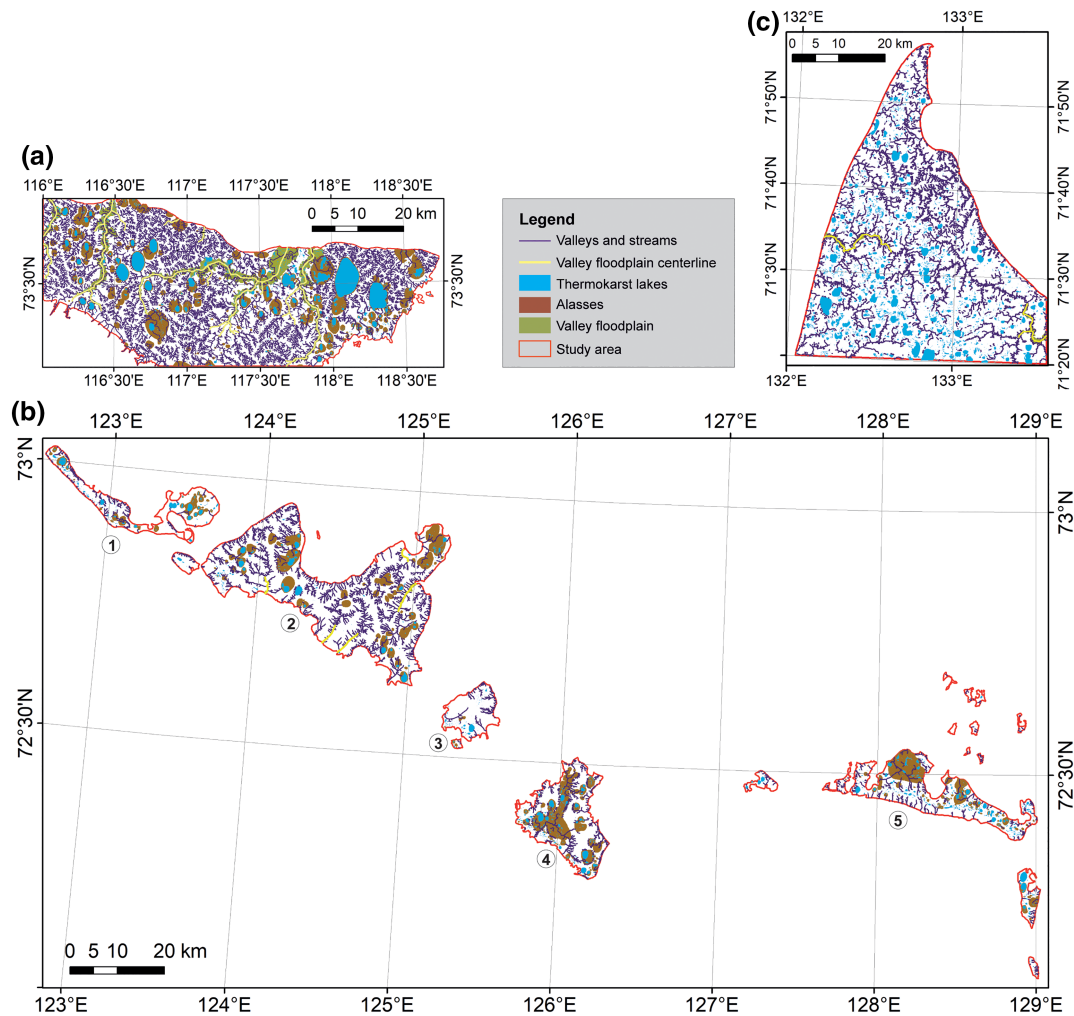


**FIGURE 2** Overview of all digitized thermo-erosional and thermokarst landforms in the study areas. (a) Cape Mamontov Klyk; (b) Lena River Delta area: 1 – Ebe-Basyn Island, 2 – Khardang Island, 3 – Dzhangylakh Island, 4 – Kurungnakh Island, 5 – Sobo-Sise Island; (c) Buor Khaya Peninsula [Colour figure can be viewed at [wileyonlinelibrary.com](http://wileyonlinelibrary.com)]

4. Another type of V-shaped valley is the small tributary type described in section 4.2 (Table 3d, Figure 4d). They are much wider (up to hundreds of meters) than the V-shaped ravines (tens of meters wide) and longer (hundreds of meters) and therefore have more gentle slopes in cross-section and a moderate to low gradient in longitudinal profile.

5. U-shaped valleys are widely distributed in the study areas (Table 3e, Figure 4e). Their cross profiles are characterized by steep slopes that transition abruptly to a flat valley floor, which can be several tens of meters wide (Figure 5d). These valleys often follow the polygonal network and can bend at 90° angles.

6. The larger type of U-shaped valley (Table 3f, Figure 4f) is much wider with more gentle slopes in cross profile and occupied by permanent streams.

7. Broad valleys with fluvial floodplains are found in the lower elevation regions of the Cape Mamontov Klyk and Buor Khaya Peninsula study areas close to the coast. The streams and rivers in these valleys meander with high sinuosity (Table 3g, Figure 4g). Transitions between these valley categories downstream are common, but they are not exclusively unidirectional and smooth. In the Cape Mamontov Klyk area we

observed, for example, a meandering valley with a U-shaped profile and a small stream in the upper valley section that abruptly transitioned into a V-shaped ravine with disturbed soil and vegetation cover at the location of a rapid drop in elevation (Figure 5b).

In addition to these different valley landforms, we also observed parallel water tracks on slightly inclined Yedoma uplands and alas floors (Table 3h). These water tracks are not included in our analyses, because they are not or are only slightly incised into the surface. Similar features have been described for hill slopes in other regions and are sometimes referred to as dells.<sup>31,68–72</sup>

## 5 | DISCUSSION

### 5.1 | Data accuracy

The geo-dataset of thermo-erosional landforms analyzed in this study was compiled using existing datasets that had been mapped based on topographical maps and satellite imagery with differences in spatial

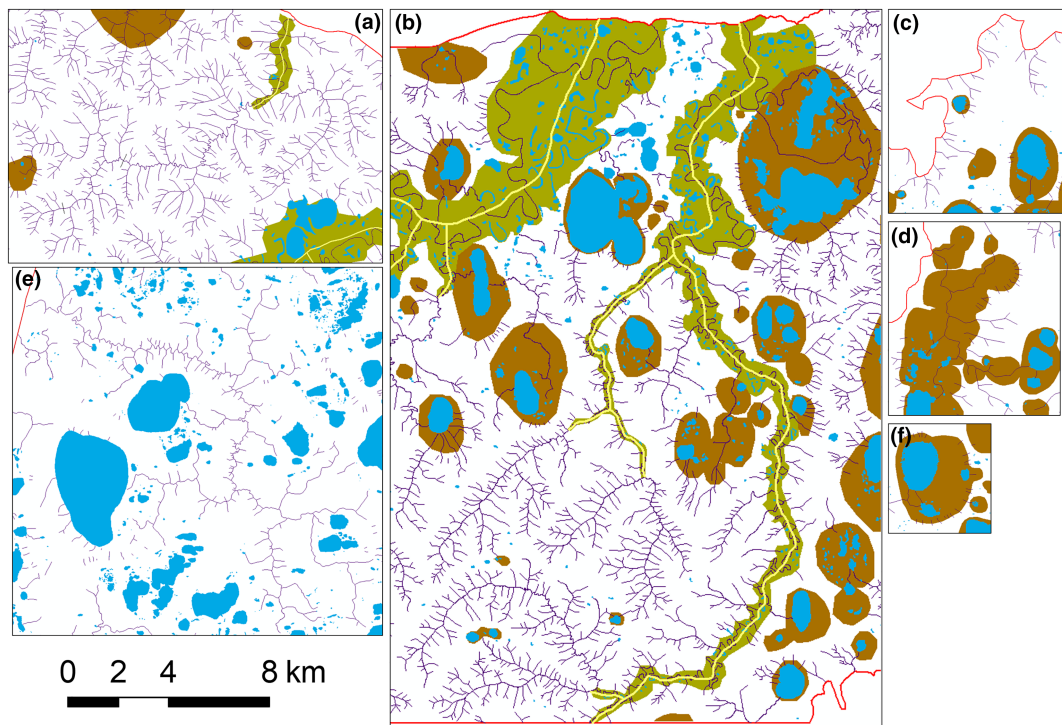


**FIGURE 3** Examples of different drainage patterns in the study area: (a) extensive dendritic valleys, Cape Mamontov Klyk; (b) extensive valley networks with irregular drainage patterns including dendritic, pinnate, and trellis-like forms, Cape Mamontov Klyk; (c) short parallel valleys along the ice complex margin, Lena River Delta; (d) drainage pathways in alasses, Lena River Delta; (e) extensive valleys with sharp meanders and short contributing valleys, Buor Khaya Peninsula; (f) straight, short radial gullies around thermokarst lakes and on alas slopes, Lena River Delta. For legend see Figure 2 [Colour figure can be viewed at [wileyonlinelibrary.com](http://wileyonlinelibrary.com)]

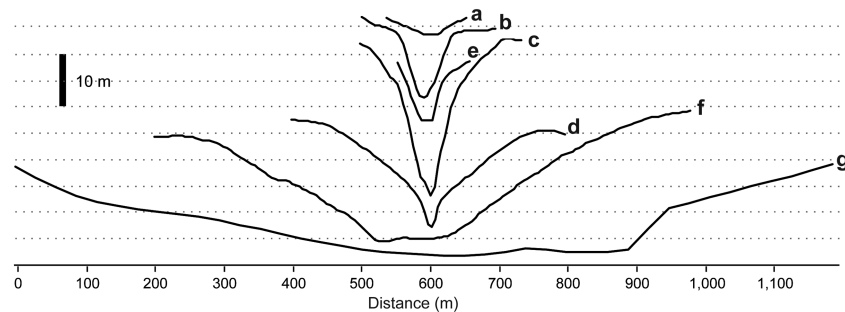


**FIGURE 4** Examples of transverse profiles of different valley types extracted from the ArcticDEM (letters correspond to the categories in Table 3; category (h) is not shown because of their shallow depth): (a) short, straight gully on alas slope; (b) drainage pathway in alas; (c) V-shaped ravine; (d) V-shaped valley with a straight thalweg of an intermittent stream; (e) U-shaped valley with a straight thalweg of an intermittent or small permanent stream; (f) U-shaped valley with a meandering thalweg of a permanent stream; (g) broad valley floodplain with a large meandering river and small oxbow and thermokarst lakes

resolution and acquisition times between the study areas (Table 1). Due to this heterogeneity of the dataset, we cannot entirely exclude differences in the degree of mapping completeness and hence the representation of the lateral extent of thermo-erosional landforms between the three study areas. In this case, these differences would have propagated into the results of the analyses of spatial metrics for a particular area, such as total stream length or drainage density (Table 2). Regarding the subsequent comparison between the study areas, in an unfavorable case this could have added up to

inconsistencies with the potential to decrease the validity of this cross-area comparison. However, we consider these effects to be minimal for the following reasons.

The best ground resolution of the satellite data used as a basis for the mapping of thermo-erosional landforms was 10 m for the Cape Mamontov Klyk and Lena Delta areas and 6.5 m for the Buor Khaya Peninsula. This ground resolution sufficiently allowed for the detection of all major thermo-erosional landforms analyzed in this study. Even though landforms of the smaller categories can be <10 m wide

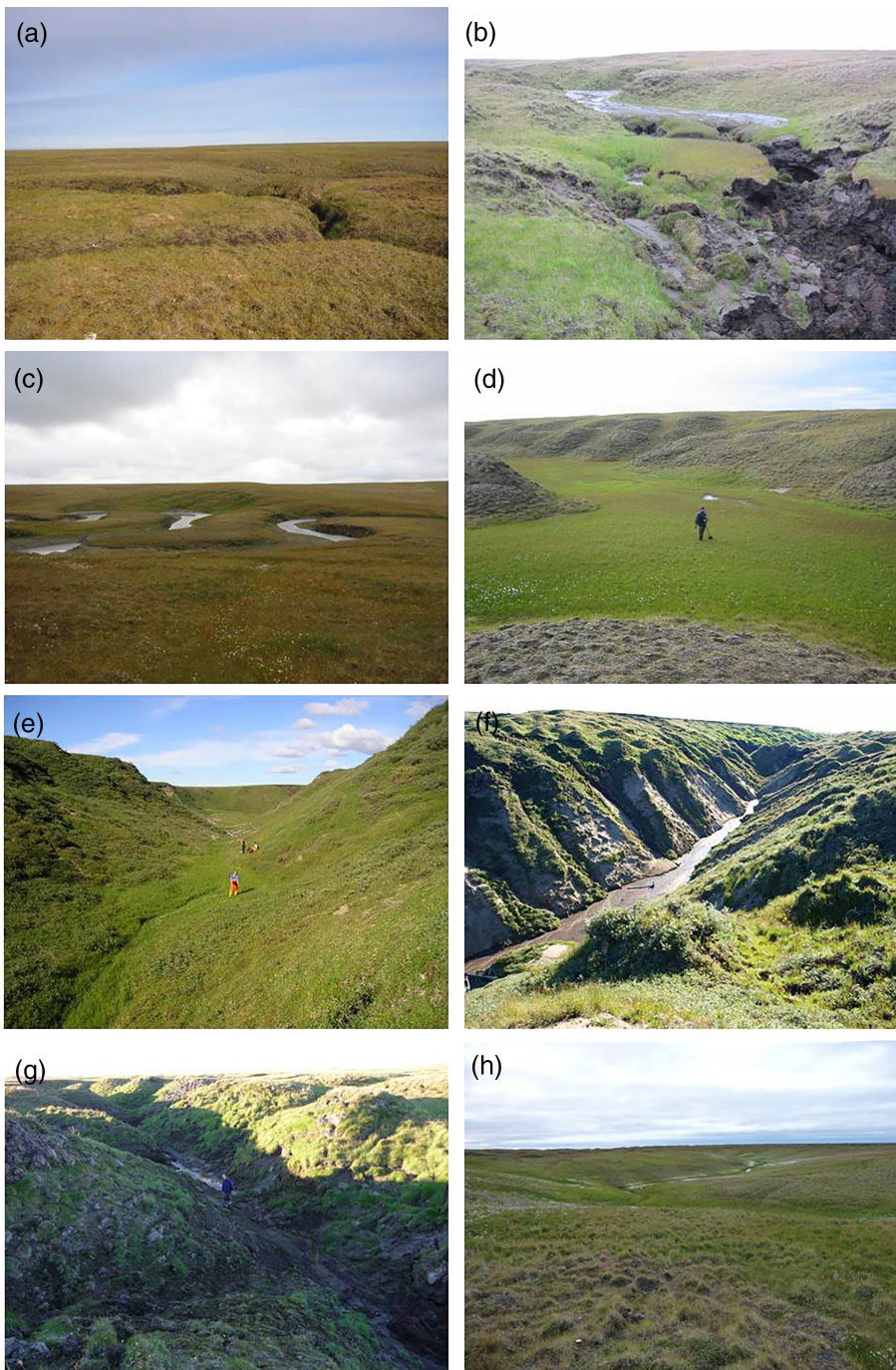


**FIGURE 5** Examples of gullies, valleys, and streams on Cape Mamontov Klyk (a–d), Kurungnakh Island, Lena Delta (e, f), and Buor Khaya Peninsula (g, h). (a) Gully initiation due to melting polygonal ice wedges. (b) Erosion and disturbed vegetation cover due to strong discharge in an intermittent stream. (c) Strongly meandering permanent stream that is eroding the ice-rich permafrost along the outer banks. (d) U-shaped valley with a broad, flat, densely vegetated floor and little surface water flow. (e) V-shaped valley on the floor of a large alas that formed when the primary thermokarst lake was tapped by the neighboring delta channel. The lake drained catastrophically and washed away the unfrozen, predominantly sandy sediments from the lake bottom into the delta channel, whose water level was several meters below the lake floor. (f) Deep, V-shaped valley that retrogressed into the permafrost and drained a small thermokarst lake between 1975 and 2000. Slopes in the lower stratigraphic sand unit are much steeper and less vegetated than in the upper Yedomia Ice Complex unit, where baydzharakhs are present. See log on valley floor for scale. (g) V-shaped valley with small side valleys along polygonal ice wedges and disturbed vegetation cover on the floor and lower parts of the slopes. Position is about 150 m from the coast. (h) Smoothly meandering valley with gentle slopes [Colour figure can be viewed at [wileyonlinelibrary.com](http://wileyonlinelibrary.com)]

(Table 3), they are in most cases still recognizable in satellite imagery of 10-m ground resolution due to mixed-pixel effects caused by the differing spectral reflectance between the two opposite slopes of the landforms and between the slopes and the surrounding surface. This effect was the reason for the main mapping criterion being the clear incision of the landform into the surface, which we introduced in the Methods section.

Topographic maps were the coarsest-resolution dataset and were expected to have some degree of generalization. They were the initial mapping basis for the hydrological features in the Cape Mamontov Klyk area. Subsequently, satellite data were used for mapping smaller

gullies and valleys not captured in the topographic maps. A small portion of the western study area was not covered by the Hexagon imagery (10-m resolution), only by the Landsat imagery (15-m resolution). However, because the highest drainage density was observed around Cape Mamontov Klyk, any higher resolution datasets here would have increased not only the drainage density metric for the site, but even more would have pronounced the differences to the other sites. On the Buor Khaya Peninsula, a low drainage density was observed based on consistent high-resolution RapidEye imagery (6.5 m), resulting in a high degree of mapping completeness. If we had applied similar coarser resolution datasets as in the other study areas also here, it

**TABLE 3** Categories of thermo-erosional valley landforms and hydrological features based on field observations and spatial analyses in the study region

Landform	Occurrence	Gross profile	Longitudinal profile/gradient	Typical width	Typical depth	Vegetation cover	Hydrologic regime
(a) Short, straight gullies	Radially arranged around lakes and alasses on their slopes	V- to U-shaped	High gradient	Up to 100 m	Up to 10 m	Dense, vital vegetation	Intermittent streams
(b) Drainage pathways in alasses	On alas floors; connect residual and secondary thermokarst lakes in partly drained alasses with the stream network outside the alasses or are remains of catastrophic lake drainage	V- to U-shaped	Low gradient	A few meters to 200 m	Up to 20 m	Dense, vital vegetation	Intermittent and small permanent streams
(c) V-shaped ravines	Along steep coasts and cliffs; sometimes due to lake drainage	V-shaped	High gradient	Up to 200 m	Tens of meters	Vegetation cover on floor and lower slopes often disturbed	Intermittent streams
(d) V-shaped valleys	In upper parts of the watersheds on Yedoma uplands, mostly tributary valleys	V-shaped	Moderate to low gradient	Hundreds of meters	Several to tens of meters	Intact vegetation cover	Intermittent streams
(e) U-shaped valleys	On Yedoma uplands	U-shaped with steep slopes and flat valley floor	Moderate to low gradient	Several to tens of meters	Up to 10 m	Dense, vital vegetation	Intermittent and small permanent streams
(f) U-shaped valleys of permanent streams and rivers	Lower parts of long streams close to their mouth	U-shaped	Low gradient	Hundreds of meters	Up to tens of meters	Dense, vital vegetation	Permanent, meandering streams
(g) Broad valley floodplains	Lower parts of long streams/rivers close to their mouth	Broad floors with distinct floodplains with oxbow and small thermokarst lakes	Low gradient	Hundreds of meters to kilometers	Up to tens of meters	Dense, vital vegetation, sometimes bare sediment exposed	Permanent, meandering streams
(h) Water tracks	Arranged in parallel; on gently sloping Yedoma uplands; on large, slightly inclined alas floors	Not or only slightly indented into the surface	Low gradient	Up to a few meters	Decimeters	Dense, vital vegetation	Poorly developed runoff systems

would have decreased the drainage density for the Buor Khaya site, thus further emphasizing differences between the study sites.

Our field observations indicate that the only thermo-erosional landforms not readily detected with these datasets are fresh gullies that were developing along the polygonal network by melting of ice wedges but had not yet eroded the adjacent sediments and therefore had not developed slopes. Such gullies are constrained to actively eroding source zones of currently developing and/or expanding thermo-erosional valleys and usually extend less than a few tens of meters in length. We estimate that these thermo-erosional landforms below the detection limit of this study account for less than 1% of thermo-erosional landforms in the study region. This estimation is supported by a change detection study, which analyzed the lateral expansion of thermo-erosional valleys for parts of the Lena Delta study site based on Hexagon data from 1975 and RapidEye data from 2010/2011.<sup>73</sup> This study found lateral changes of about 1.3%. In addition, this change detection study supports the assumption that the proportion of thermo-erosional landforms that developed after the Hexagon acquisition date, but could not be detected in the more recent Landsat imagery because of its coarser ground resolution, is negligible. A change in total stream length by +1% would change the drainage densities only in the second decimal place for all three study areas. However, increased activation of thermo-erosional processes can be expected under Arctic warming, and future investigations should take advantage of satellite imagery of higher ground resolution that are recently becoming increasingly available for the Arctic region.

## 5.2 | Conceptual models of valley formation and evolution

In the following, we propose conceptual models of the formation and evolution of thermo-erosional landforms in the study region. In the first part, we focus on the individual valley categories that we distinguished in section 4.3 and which occur in all three study areas. In the second part, we discuss the factors and conditions that led to regional differences in the evolution of the study areas and their valley networks.

### 5.2.1 | Valley categories

The short, straight gullies on the slopes of thermokarst lakes and alasses (Figure 3f, Table 3a) form due to concentrated surface runoff from the Yedoma uplands into the lakes and alasses. Sediments are transported down slope and can form small alluvial fans on alas floors.<sup>35</sup> Snow accumulating in gullies, niches, and valleys promotes further erosion, because it insulates the permafrost from low temperatures during winter and supplies more runoff during snowmelt in spring. This nivation feedback is also important for all other valley types described in this study.

The drainage pathways in alasses (Figure 3d, Table 3b) as well as a large percentage of the streams on the degraded surface of the Buor

Khaya Peninsula (Figure 3e) are either primary pathways created during the drainage of thermokarst lakes or secondary pathways that formed after permafrost aggradation in alasses. Figure 5e shows a very large and deep example of the first drainage pathway type. It formed by eroding as deep as 10 m into the unfrozen sediments of a suddenly drained large lake. The second type often forms along Holocene polygonal ice-wedge networks on alas floors when precipitation and snowmelt water collects in polygon troughs and discharges to lower elevation areas and into larger drainage streams and valleys. Similar polygon-assisted stream incisions were also observed because of the changing hydraulic conductivity of polygon wedges vs. interiors, in addition to the topographic driver.<sup>74</sup> The polygon troughs widen, and in cases where small ponds form at polygon junctions, beaded drainage occurs.<sup>3,35</sup> Larger streams further erode the alas floor so that they are no longer confined to the ice-wedge polygon network, creating smoothly meandering valleys with gentle slopes and without back-wasting by polygon block failure (Figure 5h), but evolving similarly to the other permanent streams in the study areas as described below.

V-shaped ravines at steep Yedoma cliffs (Figure 3c, Table 3c) are shaped by rapid headward erosion. They initiate at small incisions in cliff edges often where large ice wedges melt, and erosion is reinforced due to accumulating snow and melt water runoff until they stabilize and transform to other morphological valley types when approaching equilibrium between erosion and sedimentation. Headward erosion occurs along the ice-wedge network at rates of up to several tens of meters per year.<sup>14</sup> Such ravines propagate inland and may tap thermokarst lakes, leading to abrupt drainage and resulting in strong deepening and widening by thermal erosion during the drainage event (Figure 5f). When erosion slows down they become completely vegetated.

The V-shaped valleys (Table 3d), U-shaped valleys (Table 3e), and valleys of permanent streams (Table 3f) are usually part of extensive valley networks and evolve as an interdependent hydrologic system. Their development on the slightly inclined surface of the Yedoma uplands starts from slight depressions that concentrate the intermittent surface runoff, such as water tracks or dells (Table 3f). Due to active layer deepening and sediment outwash by the running water, which can be considerable even with the vegetation cover remaining intact, the water tracks and depressions deepen further, thereby creating V-shaped valleys with long, slightly inclined slopes (Figure 4d). In areas of higher relief, valley initiation can also occur by gullying along polygonal ice-wedge systems. Due to the confluence of several valleys, more water accumulates downstream, so that further valley development is characterized by an intensification of the erosion laterally as well as to depth, but nivation and solifluction may even play a more effective role in the lateral erosion and widening of the valleys. As a result, the valley shapes transform from V to U.

Finally, when large permanent streams become meandering rivers, broad floodplains develop. One scenario is when the erosional base rises in the course of sea transgression or tectonic downward movements, decreasing flow velocities and incision intensity while

enhancing valley widening through bank cutting. In addition, larger rivers in the Mamontov Klyk area (Urasalakh River) have their source in a mountain ridge with exposed bedrock and may therefore have a braided stream origin. Once coarse sediment supply ceases, braiding intensity decreases, and distinct channels form.<sup>75</sup> In the case of abrupt elevation changes, for example at the junctions of streams or valleys of different orders, valley transverse profiles can change from one type to another. Figure 5b shows such an example, where a steep V-shaped ravine is retrograding into a small and shallow U-shaped valley.

## 5.2.2 | Evolution of the valley networks

The study areas differ greatly in terms of drainage patterns and densities as well as in the distribution of the different valley categories and thermokarst landforms, even though they all represent Yedoma Ice Complex settings. This implies that factors and conditions governing valley evolution and Yedoma Ice Complex degradation must have affected the study areas differently. Here we propose a conceptual model including regional landscape evolution and site-specific development that led to the present-day valley network characteristics (Figure 6).

In the study region, development of the modern hydrological system began with the Lateglacial/early Holocene transition period, when accumulation of the Yedoma Ice Complex deposits ceased and the regional climate shifted to warmer and wetter conditions, promoting the activation of rivers and widespread permafrost degradation.<sup>31,34,46–48,58</sup> The coastline of the Laptev Sea was located several hundred kilometers further north during that period,<sup>76</sup> and extensive ice-rich permafrost lowlands with low gradients provided favorable conditions for thermokarst (Figure 6a).

Thermokarst processes slowed down substantially with mid- to late Holocene cooling<sup>35,58,77</sup> and the transgressing Laptev Sea reached its modern position about 5 cal. ka BP (Figure 6b).<sup>76</sup> While the transgressing shoreline caused lower gradients for the study area regionally, higher gradients developed locally along the coasts due to wave abrasion and coastal erosion. Steep slopes around thermokarst lakes and basins developed during subsidence tens of meters deep into the Yedoma Ice Complex surface. Both processes provided steeper gradients over shorter distances, fueling more extensive valley formation.<sup>22,78,79</sup> This is most clearly expressed at Cape Mamontov Klyk, where a steep cliff up to 30 m high was formed by coastal erosion (Figure 6c). In the Lena Delta, the Yedoma surface was cut off from the mountain ranges to the south as well as from the accumulation plains to the north by large deltaic channels and has been eroded into small disconnected remnants. They are now elevated up to 66 m above deltaic streams and floodplains, with higher relief in the western than in the eastern delta (Figure 6d).<sup>44,47</sup> The Buor Khaya Peninsula was strongly affected by thermokarst processes, which degraded a large proportion of the Yedoma Ice Complex deposits (85–90% of total area),<sup>80</sup> leaving only remnants of undisturbed Yedoma uplands on a low-elevation plain (Figure 6e). We argue that

this marked difference between the western and eastern region reflects neotectonic activity (Figure 6b).

The study region is seismotectonically very active, because it is located at the zone of intense deformation between the North American and Eurasian plates,<sup>81,82</sup> which transforms from extension in the Laptev Sea to transgression further south.<sup>83–85</sup> Modern seismicity records<sup>86</sup> show particularly high concentrations of earthquake epicenters with magnitudes of up to 5 along the Olenyokskaya and Bykovsky channels bordering the Lena Delta to the south. In the Lena Delta, a dichotomy between uplift in the western and subsidence in the eastern part has been inferred from stratigraphic investigations.<sup>33,45</sup> Tectonic movements of high amplitudes (30 m and more) are reported for the Holocene.<sup>87</sup> Khardang Island, which is the largest island of the third Lena Delta terrace, has an elevated central part in the east originating from block uplift.<sup>33</sup> The differing land surface inclinations of other islands of the third terrace also indicate neotectonic movements since at least the late Pleistocene. We assume a consistent inclination from the mountain ranges to the sea for the original late Pleistocene accumulation plain, i.e. from SSW (high) to NNE (low). The erosional remnants of this accumulation plain, which today form the third Lena Delta terrace, should in general show the same inclination. However, the planar surface of the Yedoma upland of Kurungnakh Island is inclined from SE to NW and the surface of Dzhangylakh Island from NNE to SSW. Khardang Island shows an even more complex situation with its central block uplift in the eastern part and an inclination from N to S in the western part of the island. The Buor Khaya Peninsula is situated in an area of subsidence, the Omoloi Graben, and therefore provides conditions similar to the eastern subsiding Lena Delta sector, whereas the Cape Mamontov Klyk area is situated in the Lena–Taimyr Uplift and is comparable to the third terrace islands in the western Lena Delta section.<sup>81</sup>

Previous studies reported that in regions of tectonic uplift, permafrost degradation creates distinct landforms that are deeply incised into the ice-rich deposits, and thermal erosion dominates over thermokarst, whereas the surface in lowered regions degrades almost completely and predominantly by thermokarst.<sup>58,88</sup> We can confirm this statement for our study region in which the characteristics of the degradational landforms and the present-day elevation represent an uplift situation in the western part of the study region and a subsidence situation in the eastern part. At Mamontov Klyk, degradational landforms are deeply incised into the Yedoma surface, and thermo-erosional valleys dominate the area, even though very large thermokarst lakes and alasses also exist (Figure 2). On the Buor Khaya Peninsula, only a few isolated Yedoma uplands remain and current thermo-erosional valleys mainly occur on the flat lowland surfaces that resulted from extensive degradation by thermokarst. In the Lena Delta, the situation on Khardang Island resembles that in the Cape Mamontov Klyk area, while the characteristics of the eastern delta are similar to those on the Buor Khaya Peninsula. Our results thus corroborate the role of neotectonics for setting the context for valley network expression in ice-rich permafrost regions (Figure 6).

In addition to relief, rainfall, infiltration capacity, and other factors that influence drainage densities and valley morphometry in non-

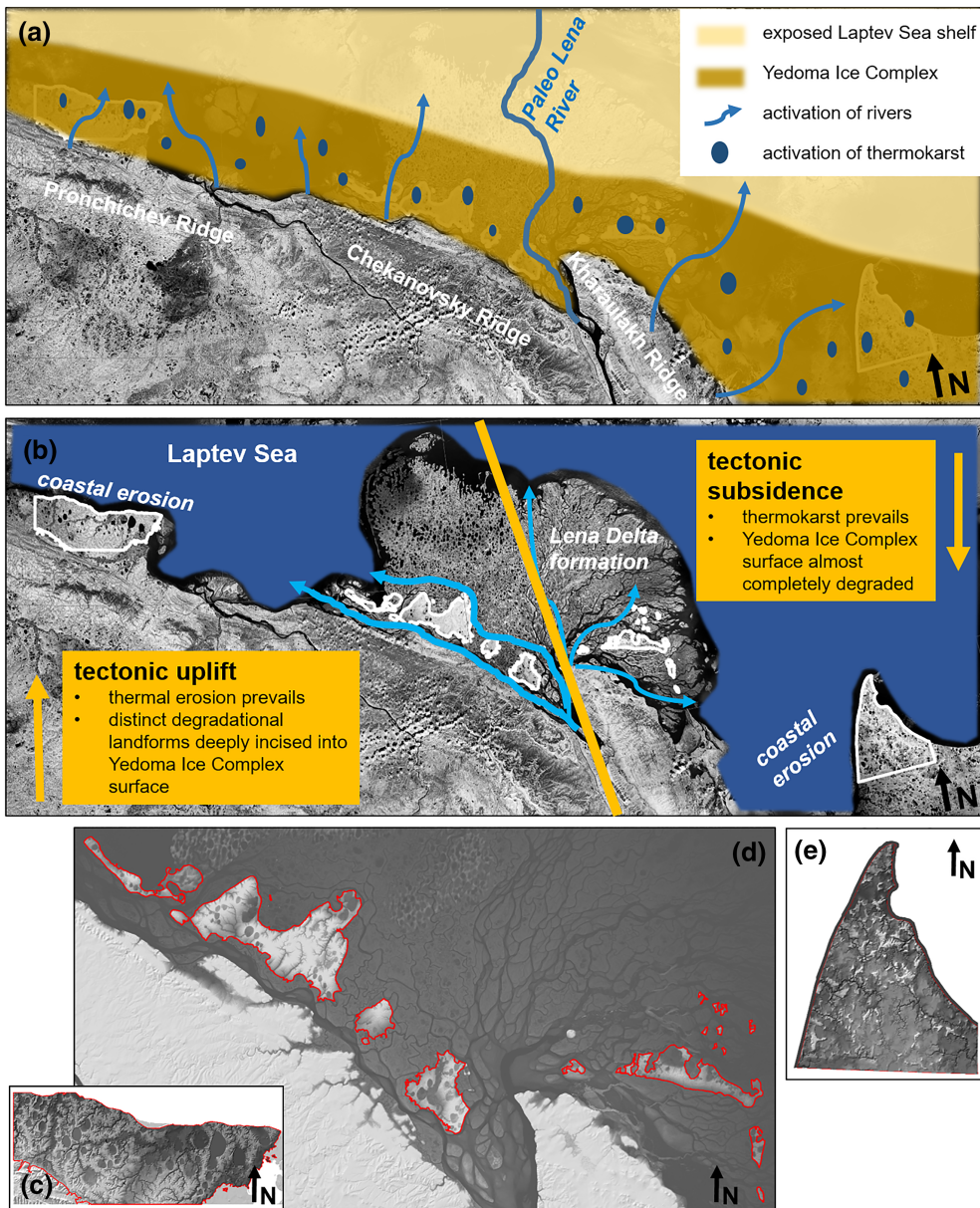


**FIGURE 6** Schematic overview of processes and conditions that governed the evolution of the study areas and their valley networks (a, b; background image Landsat-7 ETM + mosaic, GeoCover™ 2000) and resulting present-day relief situation (c–e; DEM shaded reliefs). (a) Lateglacial–Holocene transition: ceasing Yedoma Ice Complex accumulation in the foreland of mountain ranges, activation of rivers and widespread thermokarst. (b) Mid-to late Holocene: coastal erosion due to transgressing Laptev Sea, differentiation in prevailing type of permafrost degradation between western and eastern study region due to neotectonic movements, and formation of the modern Lena River Delta. (c) Cape Mamontov Klyk. (d) Lena River Delta. (e) Buor Khaya Peninsula. Note that the symbols for rivers, thermokarst, Yedoma ice complex, and exposed Laptev Sea shelf in (a) and (b) are schematic and do not represent actual locations of landforms and boundaries [Colour figure can be viewed at [wileyonlinelibrary.com](http://wileyonlinelibrary.com)]

arctic regions,<sup>60</sup> ground ice plays an important role in ice-rich permafrost lowland regions. Besides providing the preconditions for thermokarst and thermal erosion, its distribution influences stream and valley formation and evolution.<sup>89</sup> Thermal erosion along polygonal ice-wedge systems, for example, results in the formation of zigzag-shaped streams.<sup>3,14</sup> Linear thermal erosion also plays an important role in the sediment transport down slope, including intermittent streams that are only active during the short summers. The large inflow of talus deposits and solifluction material from the slopes supports the dominance of lateral over downcutting erosion in the formation of larger river valleys in permafrost regions, which leads to strongly meandering rivers in wide valleys and fluvial planation through channel migration.<sup>15,90</sup>

Whereas drainage density reflects the contemporary extent of active streams, valley density is a morphometrical indicator integrating valley-forming and valley-filling processes in a study region over long

millennial time scales. It therefore accounts for environmental conditions during the formation and persistence of the valleys.<sup>91,92</sup> The modern activity of streams is reflected in the drainage density. Runoff is generated by rainfall and by melting snow and ground ice. The high number of intermittent streams contributes substantially to the drainage densities, which would be much lower if just permanent streams were considered. Because rivers and streams with large meanders only represent a small fraction of all streams mapped, the valley densities do not or only slightly differ from the drainage densities of the study areas.

The high valley density in the Cape Mamontov Klyk area (1.8) compared to the other two study areas (0.9 and 1.0 in the Lena Delta and on the Buor Khaya Peninsula, respectively) indicates that fluvial and thermal erosion found more favorable preconditions for incision into the Yedoma Ice Complex deposits here. At the same time, substantial valley formation limited lake formation and enhanced drainage

of existing thermokarst lakes before they may have occupied larger fractions of the region (Table 2). This implies that dense valley formation may support protection of Yedoma Ice Complex degradation from deep thermokarst activity, a finding supporting previous results from landscape-scale thermokarst lake modeling.<sup>36</sup> Minimum distances between the highest and lowest elevation point in each study area are longest on Cape Mamontov Klyk (22 km compared to 7 km in the Lena Delta and on the Buor Khaya Peninsula); it is the largest study area, and represents a homogeneously inclined surface from the mountain ranges to the coast. Runoff here takes place over distances of tens of kilometers. In addition, valley heads and their watersheds are not exclusively situated inside the study area, but start in the Pronchishchev Ridge, whose runoff is added to the water supplied by precipitation and melt water from thawing permafrost within the study area. This water source continues to affect the area, as evident from the much larger areal extent of valley floodplains with mostly meandering permanent streams and rivers on Cape Mamontov Klyk and from the higher values of drainage density compared to valley density (Table 2).

In the Lena River Delta study area, valleys are predominantly short (up to 2 km long) and rarely form extensive networks. They are aligned along the steep cliffs of the small islands and cut deep into the Yedoma Ice Complex and underlying sands along large ice-wedge systems perpendicular to the islands' margins. This pattern confirms that valley formation on the Lena Delta Yedoma uplands must have occurred after they were cut off from the hinterland by delta channels and do not represent residual fractions of previously existent valleys. Due to the short distances between the interior of the Yedoma islands and their margins (<10 km), the valleys follow a high gradient, which favors erosion. On the other hand, the watersheds are small and thus the supply of running surface water as an eroding agent on the Yedoma uplands is very limited. For the same reason, larger streams are rare, which is also reflected by the smallest valley floodplain area of all three study areas (8.2 km<sup>2</sup>) and by the smallest maximum floodplain width (1 km) (Table 2). Modern changes in the thermo-erosional valleys are stimulated by erosion from actively shifting deltaic channels, where the channels either erode the islands' margins<sup>93</sup> or accumulate new sediment in front of islands.

On the Buor Khaya Peninsula, the surface of the study area is slightly inclined from the water divide in the center to the Buor Khaya Bay coast in the east and the Yana Bay coast in the west; steep gradients are only found around the Yedoma remnants. Therefore, the majority of the streams do not occupy deep valleys in thick Yedoma Ice Complex deposits, but cut a few meters deep into the lower surfaces previously degraded by thermokarst. Most of them probably do not indicate the location of former valleys that had formed on the Yedoma uplands during the Lateglacial/early Holocene transition, because they are either drainage channels of thermokarst lakes or formed on refrozen extensive and nested alasses as drainage pathways through flat, low-elevation areas. This is also supported by the trellis or rectangular-like drainage pattern that predominantly follows the polygonal pattern of Holocene permafrost deposits. In contrast to the Cape Mamontov Klyk area, where additional water is supplied

from the Pronchishchev Ridge, discharge on the Buor Khaya Peninsula originates from local precipitation and melting ground ice only. Water supply is therefore limited in a similar fashion to that in the Lena Delta area. However, on the Buor Khaya Peninsula longer permanent streams and even rivers and larger floodplains exist, which can be explained by the lower overall gradient of this study area compared to the Lena Delta.

We conclude that the characteristics of the present-day valley networks in the study region reflect the climate and relief conditions, including neotectonics, during the middle and late Holocene. This is supported by late Holocene radiocarbon ages of valley fillings on Cape Mamontov Klyk.<sup>46</sup> The present-day cryolithology of the study areas is also a result of the described relief situations. The widespread thermokarst development in the lowered regions led to the thawing and compaction of the Yedoma Ice Complex deposits over extended areas, with a lower ice volume at the landscape scale. Even though aggrading Holocene permafrost on these degraded surfaces can also be ice-rich, the large ice volume of the late Pleistocene deposits as well as their initial surface level is not reached. In the uplifted areas, thermal erosion has been the dominant type of permafrost degradation. In the valleys, the Yedoma Ice Complex has thawed and much of the sediment eroded, and in alasses, the Yedoma Ice Complex deposits have been transformed similarly to those in the lowered regions. Largely undegraded Yedoma uplands remained in some areas that still feature the original late Pleistocene deposits with high ice contents.

The altered cryolithological conditions in degraded parts of the landscape considerably influence the morphometric characteristics of subsequently evolving degradational landforms. Newly developing thermokarst and thermo-erosional processes are generally restricted in depth because of the lower total ice volume.<sup>34,35</sup> Lakes in alasses have maximum depths of about 4 m, while alasses themselves are up to 35 m deep.<sup>34</sup> Similarly, thermo-erosional valleys in degraded areas are up to about 10 m deep, while those that have incised into Yedoma surfaces reach maximum depths of 35 m. Thermo-erosional valleys that form on Yedoma uplands mostly follow a steeper gradient and develop dendritic networks, whereas streams that drain flat degraded surfaces follow a more longitudinal course over small gradients.

In a warming Arctic with active-layer deepening<sup>94</sup> and precipitation regime shifts,<sup>95</sup> permafrost degradation is expected to increase. The consequences of this increase include more thermal erosion and thermokarst, intensified organic matter cycling, and release as well as shifts in the seasonality and intensity of the hydrological regime.<sup>10,96</sup> In the landscapes analyzed in this study, this will lead to an expansion of the stream and valley networks and enhanced thermokarst dynamics, including lake formation and drainage with subsequent permafrost aggradation. Re-activation of degradation processes on previously degraded surfaces will potentially have a greater share than those on Yedoma uplands. Further lateral expansion of thermo-erosional landforms on undisturbed Yedoma surfaces requires a change in the base level of erosion, wherever the existing hydrological network has reached a stable state with respect to the local and regional relief conditions. Future changes of the baseline of erosion are possible as a

result of thermokarst lake drainage and thaw subsidence, changes in the course of the river channels in the Lena Delta affecting the borders of the Yedoma remnants, coastal erosion, sea-level rise, and neotectonic activity.

## 6 | CONCLUSION

Valley and stream networks in East Siberia reflect the late Holocene development of the regional hydrological system in extensive coastal lowlands. They developed in more pronounced relief that formed due to the eroding effects of the transgressed Laptev Sea, delta channels, and thermokarst subsidence. The morphology and spatial distribution of the valley systems vary greatly from west to east and depend on the (a) regional slope, (b) size of the catchments, and (c) previous degradation of the initial Yedoma Ice Complex surface by thermokarst.

In the Cape Mamontov Klyk area, extensive valley networks of dendritic, pinnate, and trellis-like patterns have formed on a broad Yedoma Ice Complex plain between the Pronchishchev mountain range and the Laptev Sea. Large catchments and runoff from this mountain range led to the formation of permanent rivers and deeply incised valleys, which also prevented formation of widespread thermokarst lakes. In the Lena River Delta, predominantly short, but deep valleys have steeply incised into the small Yedoma Ice Complex remnants, and extensive networks occur only on the largest island Khardang. Streams and valleys on the Buor Khaya Peninsula mainly evolved on low surfaces that had been degraded by extensive thermokarst. The valley networks display an irregular pattern with long main valleys and short tributaries, which often follow the ice-wedge polygonal pattern of the degraded surfaces.

Differences in topography and the predominance of one type of permafrost degradation, thermokarst or thermal erosion, over the other can partly be attributed to neotectonic activity. In the elevated areas of the western part of the study region thermo-erosional landforms dominate the landscape and the original Yedoma Ice Complex surface between the degradational landforms has mostly been preserved, while in the lowered eastern parts it has been almost completely eroded, mainly by thermokarst.

The valley formation processes in all three study areas were strongly influenced by the thermal erosion of juvenile ice-rich, fine-grained permafrost deposits, on the original Yedoma Ice Complex land surface as well as in the secondary polygonal tundra of thermally degraded and mechanically reworked surfaces. The abundance of valleys and streams shows that thermal erosion played a key role in past degradation. Most of the valleys that developed during the late Holocene appear largely stabilized, but thermal erosion continues to be active today. Under continued Arctic warming with increasing permafrost temperatures, active layer depths, and changing precipitation patterns, thermal erosion might substantially contribute to further degradation of ground ice-rich permafrost landscapes. On the other hand, the existing valley network also has stabilizing effects on the tundra landscape, such as leveling of gradients and inhibition of thermokarst processes by enhancing lake

drainage. Therefore, in addition to better-known thermokarst landforms such as lakes and basins, existing thermo-erosional valley landforms and their further development have the capacity to affect biogeochemical and hydrological cycling of large Arctic regions by triggering events, controlling their magnitude, and moderating their timing.

## ACKNOWLEDGEMENTS

We thank S. Lange for post-processing of the 2017 GNSS data and K. Anders for field assistance. The logistical support of the fieldwork by the Russian-German Expeditions LENA and by the Research Station "Samoylov Island" operated by the Trofimuk Institute of Petroleum Geology and Geophysics, Siberian Branch, Russian Academy of Sciences, is greatly appreciated. RapidEye imagery was kindly provided by DLR through the RapidEye Science Archive (RESA) and DEMs by the Polar Geospatial Center under NSF-OPP awards 1043681, 1559691, and 1542736. A.M. was supported by the German National Academic Foundation, the Christiane Nüsslein-Volhard-Foundation, and the Helmholtz Postdoctoral Program (grant number PD-003); F.G. by DAAD with funds from BMBF and the EU's Marie Curie Actions Programme, REA grant agreement #605728 (PRIME); J.R. by the Helmholtz Association through the COPER Young Investigators Group (VH-NG-801) and by a stipend from Potsdam University; M.G. by the Russian Foundation for Basic Research (RFBR) (#18-45-140057, #18-05-70091); and G.G. by ERC PETA-CARB (#338335) and BMBF KoPp (#03F0764B). We thank the reviewer J. S. Levy for his valuable comments and suggestions that helped to improve the manuscript. Open access funding enabled and organized by Projekt DEAL.

## DATA AVAILABILITY STATEMENT

The data that support the findings of this study are openly available in PANGAEA at <https://doi.org/10.1594/PANGAEA.833958>, reference number 59.

## ORCID

Anne Morgenstern  <https://orcid.org/0000-0002-6466-7571>

Pier Paul Overduin  <https://orcid.org/0000-0001-9849-4712>

Frank Günther  <https://orcid.org/0000-0001-8298-8937>

Samuel Stettner  <https://orcid.org/0000-0001-5278-7931>

Justine Ramage  <https://orcid.org/0000-0001-7481-6529>

Lutz Schirmer  <https://orcid.org/0000-0001-9455-0596>

Mikhail N. Grigoriev  <https://orcid.org/0000-0003-1997-9506>

Guido Grosse  <https://orcid.org/0000-0001-5895-2141>

## REFERENCES

1. AMAP. An Update to Key Findings of Snow, Water, Ice and Permafrost in the Arctic (SWIPA) 2017. Oslo, Norway; 2019.
2. Biskaborn BK, Smith SL, Noetzli J, et al. Permafrost is warming at a global scale. *Nat Commun*. 2019;10:264.
3. Liljedahl AK, Boike J, Daanen RP, et al. Pan-Arctic ice-wedge degradation in warming permafrost and its influence on tundra hydrology. *Nat Geosci*. 2016;9(4):312-318.
4. Farquharson LM, Romanovsky VE, Cable WL, Walker DA, Kokelj SV, Nicolsky D. Climate change drives widespread and rapid Thermokarst

- development in very cold permafrost in the Canadian high Arctic. *Geophys Res Lett.* 2019;46(12):6681-6689.
5. Zimov SA, Voropaev YV, Semiletov IP, et al. North Siberian lakes: a methane source fueled by Pleistocene carbon. *Science.* 1997;277:800-802.
  6. Walter KM, Zimov SA, Chanton JP, Verbyla D, Chapin FS III. Methane bubbling from Siberian thaw lakes as a positive feedback to climate warming. *Nature.* 2006;443:71-75.
  7. Grosse G, Harden J, Turetsky M, et al. Vulnerability of high-latitude soil organic carbon in North America to disturbance. *J Geophys Res.* 2011;116:G00K06. <https://doi.org/10.1029/2010JG001507>
  8. Schuur EAG, McGuire AD, Schadel C, et al. Climate change and the permafrost carbon feedback. *Nature.* 2015;520(7546):171-179.
  9. Olefeldt D, Goswami S, Grosse G, et al. Circumpolar distribution and carbon storage of thermokarst landscapes. *Nat Commun.* 2016;7:13043. <https://doi.org/10.1038/ncomms13043>
  10. Turetsky MR, Abbott BW, Jones MC, et al. Permafrost collapse is accelerating carbon release. *Nature.* 2019;569(7754):32-34.
  11. Chapin FSI, Sturm M, Serreze MC, et al. Role of land-surface changes in arctic summer warming. *Science.* 2005;310:657-660.
  12. Osterkamp TE, Jorgenson MT, Schuur EAG, et al. Physical and ecological changes associated with warming permafrost and thermokarst in interior Alaska. *Permafrost Periglacial Process.* 2009;20(3):235-256.
  13. van Everdingen RO. (Ed). *Multi-language glossary of permafrost and related ground-ice terms.* International Permafrost Association; 1998 (revised 2005).
  14. Czudek T, Demek J. Die Reliefentwicklung während der Dauerfrostbodendegradation. *Rozpr Českosl Ak Véd Rada Mat a Pfir, VR* 1973;83.
  15. Yershov ED. *General Geocryology.* Cambridge, UK: Cambridge University Press; 2004.
  16. Costard F, Dupeyrat L, Gautier E, Carey-Gailhardis E. Fluvial thermal erosion investigations along a rapidly eroding river bank: application to the Lena River (Central Siberia). *Earth Surf Process Landf.* 2003;28(12):1349-1359.
  17. Dupeyrat L, Costard F, Randriamazaoro R, Gailhardis E, Gautier E, Fedorov A. Effects of ice content on the thermal erosion of permafrost: implications for coastal and fluvial erosion. *Permafrost Periglacial Process.* 2011;22(2):179-187.
  18. Dupeyrat L, Hurault B, Costard F, Marmo C, Gautier E. Satellite image analysis and frozen cylinder experiments on thermal erosion of periglacial fluvial islands. *Permafrost Periglacial Process.* 2018;29(2):100-111.
  19. Kanevskiy M, Shur Y, Strauss J, et al. Patterns and rates of riverbank erosion involving ice-rich permafrost (yedoma) in northern Alaska. *Geomorphology.* 2016;253:370-384.
  20. Tananaev NI. Hydrological and sedimentary controls over fluvial thermal erosion, the Lena River, central Yakutia. *Geomorphology.* 2016; 253:524-533.
  21. Gavrilov AV, Romanovskii NN, Romanovsky VE, Hubberten HW, Tumskey VE. Reconstruction of ice complex remnants on the eastern Siberian arctic shelf. *Permafrost Periglacial Process.* 2003;14(2):187-198.
  22. Günther F, Overduin PP, Sandakov AV, Grosse G, Grigoriev MN. Short- and long-term thermo-erosion of ice-rich permafrost coasts in the Laptev Sea region. *Biogeosciences.* 2013;10:4297-4318.
  23. Jones BM, Grosse G, Arp CD, Jones MC, Walter Anthony KM, Romanovsky VE. Modern thermokarst lake dynamics in the continuous permafrost zone, northern Seward peninsula, Alaska. *J Geophys Res.* 2011;116:G00M03.
  24. Lara MJ, Chipman ML, Hu FS. Automated detection of thermoerosion in permafrost ecosystems using temporally dense Landsat image stacks. *Remote Sens Environ.* 2019;221:462-473.
  25. Veremeeva AA, Glushkova NV. Formation of relief in the regions of ice complex deposits distribution: remote sensing and GIS studies in the Kolyma lowland tundra. *Kriosfera Zemli - Earth's Cryosphere.* 2016; 20(1):14-24.
  26. Fortier D, Allard M, Shur Y. Observation of rapid drainage system development by thermal erosion of ice wedges on Bylot Island, Canadian Arctic archipelago. *Permafrost Periglacial Process.* 2007;18(3):229-243.
  27. Godin E, Fortier D. Geomorphology of a thermo-erosion gully, Bylot Island, Nunavut, Canada. *Can J Earth Sci.* 2012;49(8):979-986.
  28. Godin E, Fortier D, Coulombe S. Effects of thermo-erosion gullying on hydrologic flow networks, discharge and soil loss. *Environ Res Lett.* 2014;9(10):105010.
  29. Godin E, Osinski GR, Harrison TN, Pontefract A, Zanetti M. Geomorphology of gullies at Thomas Lee Inlet, Devon Island, Canadian high Arctic. *Permafrost Periglacial Process.* 2019;30(1):19-34.
  30. Grosse G, Schirrmeyer L, Malthus TJ. Application of Landsat-7 satellite data and a DEM for the quantification of thermokarst-affected terrain types in the periglacial Lena-Anabar coastal lowland. *Polar Res.* 2006;25(1):51-67.
  31. Grosse G, Schirrmeyer L, Siegert C, et al. Geological and geomorphological evolution of a sedimentary periglacial landscape in Northeast Siberia during the Late Quaternary. *Geomorphology.* 2007;86:25-51.
  32. Toniolo H, Kodial P, Hinzman LD, Yoshikawa K. Spatio-temporal evolution of a thermokarst in interior Alaska. *Cold Reg Sci Technol.* 2009; 56(1):39-49.
  33. Grigoriev MN. *Cryomorphogenesis of the Lena River mouth area.* Yakutsk, Russia: Permafrost Institute Press; 1993.
  34. Morgenstern A, Grosse G, Günther F, Fedorova I, Schirrmeyer L. Spatial analyses of thermokarst lakes and basins in Yedoma landscapes of the Lena Delta. *Cryosphere.* 2011;5(4):849-867.
  35. Morgenstern A, Ulrich M, Günther F, et al. Evolution of thermokarst in east Siberian ice-rich permafrost: a case study. *Geomorphology.* 2013;201(0):363-379.
  36. van Huissteden J, Berrittella C, Parmentier FJW, Mi Y, Maximov TC, Dolman AJ. Methane emissions from permafrost thaw lakes limited by lake drainage. *Nature Climate Change.* 2011;1(2):119-123.
  37. Muster S, Roth K, Langer M, et al. perL: a circum-Arctic permafrost region pond and Lake database. *Earth Syst Sci Data.* 2017;9(1):317-348.
  38. Smith LC, Sheng Y, MacDonald GM, Hinzman LD. Disappearing Arctic lakes. *Science.* 2005;308(5727):1429. <https://doi.org/10.1126/science.1108142>
  39. Kravtsova VI, Bystrova AG. Changes in thermokarst lake sizes in different regions of Russia for the last 30 years. *Earth Cryosphere - Kriosfera Zemli.* 2009;13(2):16-26.
  40. Grosse G, Schirrmeyer L, Kunitsky VV, Hubberten H-W. The use of CORONA images in remote sensing of periglacial geomorphology: an illustration from the NE Siberian coast. *Permafrost Periglacial Process.* 2005; 16(2):163-172.
  41. Bowden WB, Gooseff MN, Balsler A, Green A, Peterson BJ, Bradford J. Sediment and nutrient delivery from thermokarst features in the foothills of the North Slope, Alaska: potential impacts on headwater stream ecosystems. *J Geophys Res.* 2008;113:G02026. <https://doi.org/10.1029/2007JG000470>
  42. Harms TK, Abbott BW, Jones JB. Thermo-erosion gullies increase nitrogen available for hydrologic export. *Biogeochemistry.* 2014;117:299-311.
  43. Rowland JC, Jones CE, Altmann G, et al. Arctic landscapes in transition: responses to thawing permafrost. *Eos Trans AGU.* 2010;91(26):229-230.
  44. Schirrmeyer L, Grosse G, Schwamborn G, et al. Late Quaternary history of the accumulation plain north of the Chekanovsky ridge (Lena Delta, Russia): a multidisciplinary approach. *Polar Geogr.* 2003;27(4):277-319.
  45. Schwamborn G, Rachold V, Grigoriev MN. Late Quaternary sedimentation history of the Lena Delta. *Quat Int.* 2002;89(1):119-134.

46. Schirrmeyer L, Grosse G, Kunitsky V, et al. Periglacial landscape evolution and environmental changes of Arctic lowland areas for the last 60 000 years (western Laptev Sea coast, cape Mamontov Klyk). *Polar Res.* 2008;27(2):249-272.
47. Schirrmeyer L, Grosse G, Schnelle M, et al. Late Quaternary paleoenvironmental records from the western Lena Delta, Arctic Siberia. *Palaeogeogr Palaeoclimatol, Palaeoecol.* 2011;299(1-2):175-196.
48. Schirrmeyer L, Kunitsky V, Grosse G, et al. Sedimentary characteristics and origin of the Late Pleistocene ice complex on north-east Siberian Arctic coastal lowlands and islands - a review. *Quat Int.* 2011;241(1-2):3-25.
49. Schirrmeyer L, Schwamborn G, Overduin PP, et al. Yedoma ice complex of the Buor Khaya Peninsula (southern Laptev Sea). *Biogeosciences.* 2017;14(5):1261-1283.
50. Wetterich S, Kuzmina S, Andreev AA, et al. Palaeoenvironmental dynamics inferred from late Quaternary permafrost deposits on Kurungnakh Island, Lena Delta, Northeast Siberia, Russia. *Quat Sci Rev.* 2008;27(15-16):1523-1540.
51. Wetterich S, Overduin PP, Grigoriev M. *Russian-German Cooperation SYSTEM LAPTEV SEA: The expedition Eastern Laptev Sea - Buor Khaya Peninsula 2010.* Bremerhaven, Germany: Alfred Wegener Institute for Polar and Marine Research; 2011.
52. Winterfeld M, Schirrmeyer L, Grigoriev MN, et al. Coastal permafrost landscape development since the Late Pleistocene in the western Laptev Sea, Siberia. *Boreas.* 2011;40(4):697-713.
53. Walker DA, Reynolds MK, Daniëls FJA, et al. The circumpolar Arctic vegetation map. *J Veg Sci.* 2005;16(3):267-282.
54. Morgenstern A, Grosse G, Schirrmeyer L. Genetic, Morphological, and Statistical Characterization of Lakes in the Permafrost-Dominated Lena Delta. Paper presented at: Ninth International Conference on Permafrost. 2008; Fairbanks, Alaska, USA.
55. Günther F, Overduin PP, Makarov A, Grigoriev M. *Russian-German cooperation SYSTEM LAPTEV SEA: the expeditions Laptev Sea - Mamontov Klyk 2011 & Buor Khaya 2012.* Bremerhaven, Germany: Alfred Wegener Institute; 2013.
56. Overduin PP, Liebner S, Knoblauch C, et al. Methane oxidation following submarine permafrost degradation: measurements from a Central Laptev Sea shelf borehole. *J Geophys Res Biogeosci.* 2015;120(5):965-978.
57. Schirrmeyer L, Grosse G, Wetterich S, et al. Fossil organic matter characteristics in permafrost deposits of the northeast Siberian Arctic. *J Geophys Res.* 2011;116(G00M02).
58. Kaplina TN. Alas complex of northern Yakutia. *Earth Cryosphere - Kriosfera Zemli.* 2009;13(4):3-17.
59. Morgenstern A, Grosse G, Arcos DR, et al. *Inventory of thermo-erosional valleys and streams in three ice-rich permafrost lowlands adjacent to the Laptev Sea.* Bremerhaven, Germany: PANGAEA; 2014.
60. Horton RE. Erosional development of streams and their drainage basins; Hydrophysical approach to quantitative morphology. *Bull Geol Soc Am.* 1945;56(3):275-370.
61. Horton RE. Drainage-basin characteristics. *Trans Am Geophys Union.* 1932;13(1):350-361.
62. Schirrmeyer L, Grigoriev MN, Kutzbach L, Wagner D, Bolshianov D. *Russian-German Cooperation SYSTEM LAPTEV SEA: The Expedition Lena-Anabar 2003.* Bremerhaven, Germany: Alfred Wegener Institute for Polar and Marine Research; 2004.
63. Schirrmeyer L, Wagner D, Grigoriev MN, Bolshianov D. *Russian-German Cooperation SYSTEM LAPTEV SEA: The Expedition Lena 2005.* Bremerhaven, Germany: Alfred Wegener Institute for Polar and Marine Research; 2007.
64. Ulrich M, Grosse G, Chabrilat S, Schirrmeyer L. Spectral characterization of periglacial surfaces and geomorphological units in the Arctic Lena Delta using field spectrometry and remote sensing. *Remote Sens Environ.* 2009;113(6):1220-1235.
65. Wagner D, Overduin PP, Grigoriev M, Knoblauch C, Bolshianov D. *Russian-German Cooperation SYSTEM LAPTEV SEA: The Expedition LENA 2008.* Bremerhaven, Germany: Alfred Wegener Institute for Polar and Marine Research; 2012.
66. Overduin PP, Blender F, Bolshianov DY, Grigoriev MN, Morgenstern A, Meyer H. *Russian-German Cooperation: Expeditions to Siberia in 2016.* Bremerhaven, Germany: Alfred Wegener Institute Helmholtz Centre for Polar and Marine Research; 2017.
67. Minnesota Uo. ArcticDEM website. 2018; <https://www.pgc.umn.edu/data/arcticdem/>. Accessed July 12, 2018.
68. Mitt KL. K voprosu o prirode delley Daaldynskovo rayona (on the question of the nature of dells in the Daaldynskiy region). *Voprosy Geografii.* 1959;46:28-34.
69. Katasonova EG. Rol' termokarsta v razvitiy delley (The role of thermokarst in the development of dells). In: Katasonov EM, ed. *Usloviya i osobennosti rasvitiya merzlykh tolshch v Sibirii i na Severo-Vostoke (Conditions and special features of the formation of frozen horizons in Siberia and the Far-East).* Moscow, Russia: Publishing House AN SSSR; 1963:91-100.
70. McNamara JP, Kane DL, Hinzman LD. An analysis of an arctic channel network using a digital elevation model. *Geomorphology.* 1999;29:339-353.
71. Jorgenson MT, Shur YL, Osterkamp TE. Thermokarst in Alaska. Paper presented at: Ninth International Conference on Permafrost. Fairbanks, Alaska, USA; 2008.
72. Trochim ED, Jorgenson MT, Prakash A, Kane DL. Geomorphic and biophysical factors affecting water tracks in northern Alaska. *Earth Space Sci.* 2016;3(3):123-141.
73. Pollozek L. *Fernekundungs- und GIS-basierte Analyse der raumzeitlichen Entwicklung von Thermoerosionstätern im Lena-Delta (Remote sensing and GIS based analysis of the spatio-temporal evolution of thermo-erosional valleys in the Lena Delta).* Potsdam, Germany: University of Potsdam; 2015.
74. Levy JS, Head JW, Marchant DR. The role of thermal contraction crack polygons in cold-desert fluvial systems. *Antarct Sci.* 2008;20(6):565-579.
75. Chew LC, Ashmore PE. Channel adjustment and a test of rational regime theory in a proglacial braided stream. *Geomorphology.* 2001;37(1):43-63.
76. Bauch HA, Mueller-Lupp T, Taldenkova E, et al. Chronology of the Holocene transgression at the north Siberian margin. *Global Planet Change.* 2001;31(1-4):125-139.
77. Romanovskii NN, Hubberten HW, Gavrilov AV, Tumskey VE, Kholodov AL. Permafrost of the east Siberian Arctic shelf and coastal lowlands. *Quat Sci Rev.* 2004;23(11-13):1359-1369.
78. Günther F, Overduin PP, Yakshina IA, Opel T, Baranskaya AV, Grigoriev MN. Observing Muostakh disappear: permafrost thaw subsidence and erosion of a ground-ice-rich island in response to arctic summer warming and sea ice reduction. *Cryosphere.* 2015;9(1):151-178.
79. Grigoriev MN, Razumov SO, Kunitzky VV, Spektor VB. Dynamics of the Russian East Arctic Sea coast: major factors, regularities and tendencies. *Kriosfera Zemli (Earth Cryosphere).* 2006;10(4):74-94.
80. Arcos DR. *Classification of periglacial landforms based on high-resolution multispectral remote sensing data. A contribution to the landscape description of the north-Siberian Buor Khaya Peninsula.* Potsdam, Germany: University of Potsdam; 2012.
81. Drachev SS, Savostin IA, Groshev VG, Bruni IE. Structure and geology of the continental shelf of the Laptev Sea, eastern Russian Arctic. *Tectonophysics.* 1998;298(4):357-393.
82. Franke D, Hinz K, Block M, et al. Tectonics of the Laptev Sea region in northeastern Siberia. *Polarforschung.* 2000;68:51-58.
83. Grigoriev MN, Imaev VS, Kozmin BM, et al. *Geology, seismicity and cryogenic processes in the Arctic areas of Western Yakutia.* Yakutsk, Russia: Siberian Branch of the Russian Academy of Sciences; 1996.

84. Grachev AF. The Arctic rift system and the boundary between the Eurasian and north American lithospheric plates: new insight to plate tectonic theory. *Russian J Earth Sci.* 2003;5(5):307-345.
85. Fujita K, Koz'min BM, Mackey KG, Riegel SA, McLean MS, Imaev VS. Seismotectonics of the Chersky Seismic Belt, eastern Sakha Republic (Yakutia) and Magadan District, Russia. *Stephan Mueller Special Pub Ser.* 2009;4:117-145.
86. Engen Ø, Eldholm O, Bungum H. The Arctic plate boundary. *J Geophys Res Solid Earth.* 2003;108(B2):2075. <https://doi.org/10.1029/2002JB001809>
87. Galabala RO. New data on the composition of the Lena Delta. In: *Quaternary of Northeast Asia*. Magadan, Russia: Academy of Sciences of the USSR; 1987:152-172.
88. Kaplina TN, Kostaldyndina NK, Leibman MO. Relief analysis of the Kolyma lowlands for cryolithological mapping. In: *Formation of frozen ground and prognosis of cryogenic processes*. Moscow, Russia: Nauka; 1986:51-60.
89. Woo M. Permafrost hydrology in North America. *Atmosphere-Ocean.* 1986;24(3):201-234.
90. Murton JB, Belshaw RK. A conceptual model of valley incision, planation and terrace formation during cold and arid permafrost conditions of Pleistocene southern England. *Quatern Res.* 2011;75(2):385-394.
91. Schmidt KH. *Der Fluss und sein Einzugsgebiet (The river and its watershed)*. Wiesbaden, Germany: Franz Steiner Verlag; 1984.
92. Tucker GE, Catani F, Rinaldo A, Bras RL. Statistical analysis of drainage density from digital terrain data. *Geomorphology.* 2001;36(3-4): 187-202.
93. Stettner S, Beamish A, Bartsch A, et al. Monitoring inter- and intra-seasonal dynamics of rapidly degrading ice-rich permafrost riverbanks in the Lena Delta with TerraSAR-X time series. *Remote Sens.* 2018;10(1):51.
94. Yi Y, Kimball JS, Chen RH, et al. Characterizing permafrost active layer dynamics and sensitivity to landscape spatial heterogeneity in Alaska. *Cryosphere.* 2018;12(1):145-161.
95. Bintanja R, van der Wiel K, van der Linden EC, et al. Strong future increases in Arctic precipitation variability linked to poleward moisture transport. *Sci Adv.* 2020;6(7):eaax6869. <https://doi.org/10.1126/sciadv.aax6869>
96. Abbott BW, Jones JB. Permafrost collapse alters soil carbon stocks, respiration, CH<sub>4</sub>, and N<sub>2</sub>O in upland tundra. *Glob Chang Biol.* 2015;21(12):4570-4587.

#### SUPPORTING INFORMATION

Additional supporting information may be found online in the Supporting Information section at the end of this article.

**How to cite this article:** Morgenstern A, Overduin PP, Günther F, et al. Thermo-erosional valleys in Siberian ice-rich permafrost. *Permafrost and Periglac Process.* 2020;1-17. <https://doi.org/10.1002/ppp.2087>